



HAL
open science

Powellite-Rich Glass-Ceramics: A Spectroscopic Study by EPR and Raman Spectroscopy

T Taurines, Delphine D. Neff, B Boizot

► **To cite this version:**

T Taurines, Delphine D. Neff, B Boizot. Powellite-Rich Glass-Ceramics: A Spectroscopic Study by EPR and Raman Spectroscopy. Journal of the American Ceramic Society, 2013, pp.1-7. 10.1111/jace.12401 . cea-01120956

HAL Id: cea-01120956

<https://cea.hal.science/cea-01120956>

Submitted on 27 Feb 2015

HAL is a multi-disciplinary open access archive for the deposit and dissemination of scientific research documents, whether they are published or not. The documents may come from teaching and research institutions in France or abroad, or from public or private research centers.

L'archive ouverte pluridisciplinaire **HAL**, est destinée au dépôt et à la diffusion de documents scientifiques de niveau recherche, publiés ou non, émanant des établissements d'enseignement et de recherche français ou étrangers, des laboratoires publics ou privés.

Powellite-rich glass-ceramics: a spectroscopic study by EPR and Raman spectroscopy

T. Taurines¹, D. Neff², B. Boizot¹

(1) *Laboratoire des Solides Irradiés, UMR 7642 CEA-CNRS-Ecole Polytechnique, 91128
Palaiseau, France*

(2) *Service Interdisciplinaire sur les Systèmes Moléculaires et les Matériaux, UMR 3299
CEA-CNRS, 91190 Gif sur Yvette, France*

Abstract

The aim of this study is to better understand the incorporation of rare earth elements in glass-ceramics of nuclear interest. We synthesized glass-ceramics from glasses in the system $\text{SiO}_2\text{-B}_2\text{O}_3\text{-Na}_2\text{O-CaO-Al}_2\text{O}_3\text{-MoO}_3\text{-Gd}_2\text{O}_3$ by various heat treatments. Gadolinium is used both as a spectroscopic probe and as a minor actinide surrogate. Glass-ceramics contain only one crystalline phase in the bulk: powellite (CaMoO_4). This phase can incorporate Gd^{3+} and Na^+ ions by substitutions on the Ca site. We demonstrated that the charge compensation by Na^+ favors the rare earth elements incorporation. Moreover, the incorporated elements do not seem to be randomly distributed into the powellite structure.

Introduction

Molybdenum is known to be poorly soluble in borosilicate glasses and to easily induce phase separation during cooling processes [1, 2, 3]. Since Mo is an abundant fission product during reactions in nuclear fuel, its concentration can be problematic for high level waste conditioning [4]. Particularly, after the reprocessing of old fuel rods used in gas cooled reactors during the 20th century or when the charge load of glasses is too high (usually above 18.5 wt% of fission products and minor actinides for the French R7T7 glass).

Above its solubility limit (≈ 1 mol%), Mo can lead to the formation of crystalline phases like powellite (CaMoO_4) or Na_2MoO_4 distributed in the volume and even to the separation at the macroscopic scale of a complex phase mainly containing alkaline and alkaline-earth molybdates called the “yellow phase” [5, 6]. Na_2MoO_4 and the “yellow phase” can drastically impact the immobilization properties of the glass since they are highly soluble in water and can carry radioactive elements like ^{137}Cs . On the contrary, the powellite phase could be convenient for nuclear storage applications. Powellite has a tetragonal scheelite structure and crystallizes in the $I4_1/a$ group ($a = 5.225 \text{ \AA}$, $c = 11.433 \text{ \AA}$) [7]. This phase is of particular interest for nuclear waste immobilization since it is poorly soluble in aqueous solutions and allows to incorporate high quantities of MoO_3 in glass-ceramics [8]. Moreover, studies under external irradiation showed that it is highly resistant to amorphisation. Under a Transmission Electron Microscope (TEM) beam, powellite amorphisation begins between 10^{12} and 10^{13} Gy [9] which is a dose much higher than the one received during underground storage ($< 10^{10}$ Gy). Swift heavy ion irradiations made by Mendoza et al. [10] also showed a high resistance to amorphisation since no metamictisation has been detected by Raman spectroscopy and X-ray diffraction up to 10 dpa.

In CaMoO_4 , Ca^{2+} ions can be substituted by various elements. Indeed powellite is known to incorporate rare-earth elements and doped crystals have widely been studied for their laser performances and emission properties [11, 7]. Various insertion schemes are possible and have been reported in the literature. The most common substitution is $2 \text{Ca}^{2+} \leftrightarrow (\text{RE}^{3+}, \text{R}^+)$ with RE^{3+} a trivalent rare-earth and R^+ a monovalent ion [12, 13, 14]. This coupled substitution ensures the lattice electro neutrality and favors the dopant incorporation [15]. Other substitutions like 3Ca^{2+} by 2RE^{3+} plus a vacancy or $(\text{Ca}^{2+}, \text{Mo}^{6+})$ by $(\text{RE}^{3+}, \text{Z}^{5+})$ are also possible [12, 15]. Doped scheelite structures can exhibit a random distribution of the inserted elements [12, 16, 17] or an ordered insertion which can lead to the formation of

superstructures [12, 14, 16]. In powellite-rich glass-ceramics, the crystalline phase could act as a good host for actinides and therefore improve the immobilization properties.

For that purpose, we have developed model glass-ceramics containing monodisperse powellite crystals from glasses in the system $\text{SiO}_2\text{-B}_2\text{O}_3\text{-Na}_2\text{O-CaO-Al}_2\text{O}_3\text{-MoO}_3\text{-Gd}_2\text{O}_3$. The micro-structure was mainly controlled by various heat treatments described in the experimental methods. The obtained glass-ceramics contain powellite crystals well dispersed into the residual glass, with various size distributions and concentrations. Crystal sizes range from a few tens of nanometers to a few micrometers depending of MoO_3 content and heat treatments[18]. For nuclear waste immobilization, the partitioning ratio of radioelements between the glassy and the crystalline phases is a matter of concern. That is why this study addresses the speciation of Gd^{3+} ions in the glassy and the powellite phases by electron paramagnetic resonance (EPR) and Raman spectroscopy. At low Gd_2O_3 doping content (0.15 mol%), Gd^{3+} ($S=7/2$) is used as an EPR spectroscopic probe whereas at higher content, Gd^{3+} ions could be considered as a trivalent minor actinide surrogate mainly of Np^{3+} , Am^{3+} and Cu^{3+} . We particularly studied the effects of composition and heat treatments on the incorporation of Gd^{3+} ions into the powellite structure.

Experimental methods

Glass-ceramics preparation

For this study, we prepared glasses in the system: $\text{SiO}_2\text{-B}_2\text{O}_3\text{-Na}_2\text{O-CaO-Al}_2\text{O}_3$. Increasing amounts of MoO_3 are added, from 0.5 to 4.5 mol% in order to have a wide range in powellite concentration in the glass-ceramics. Gd_2O_3 is added at 0.15 mol% and 1 mol% contents.

(i) **Series Mxg** : $(0.9985-2x/100)(61.16 \text{ SiO}_2 - 16.28 \text{ B}_2\text{O}_3 - 12.85 \text{ Na}_2\text{O} - 3.88 \text{ Al}_2\text{O}_3 - 5.82\text{CaO}) - x \text{ CaO} - x \text{ MoO}_3 - \mathbf{0.15 \text{ Gd}_2\text{O}_3}$ (in mol%) with $x = 0, 0.5, 1.5, 2.5, 3.5$ and 4.5 .

(ii) **Series Mxg1:** $(0.99-2x/100)(61.16 \text{ SiO}_2 - 16.28 \text{ B}_2\text{O}_3 - 12.85 \text{ Na}_2\text{O} - 3.88 \text{ Al}_2\text{O}_3 - 5.82\text{CaO}) - x \text{ CaO} - x \text{ MoO}_3 - 1 \text{ Gd}_2\text{O}_3$ (in mol%) with $x = 0, 0.5, 1.5, 2.5, 3.5$ and 4.5 .

In the two series, CaO oxide was added in increasing amounts to the baseline glass composition to compensate the loss during powellite crystallization. Therefore the residual glass compositions of each series can be kept constant if all the molybdenum is incorporated into the powellite crystals.

Parent glasses were prepared by mixing desired amounts of reagent grade SiO_2 , H_3BO_3 , Na_2CO_3 , Al_2O_3 , CaCO_3 , MoO_3 and Gd_2O_3 . Each batch (~30 g) was melted at 1500°C for 3 + 2 hours before being quenched on a copper plate. Then all samples were annealed at 500°C to relieve internal stresses. The melting process was described in more details elsewhere [18]. Ceramics were elaborated with three chemical compositions: pure powellite CaMoO_4 , powellite doped with 0.015 mol% of Gd_2O_3 (later mentioned as $\text{CaMoO}_4\text{-Gd}$) and powellite doped with 0.015 mol% of Gd_2O_3 with a charge compensation (later mentioned as $\text{CaMoO}_4\text{-Gd-Na}$). The charge compensation was ensured by replacing CaO by $\frac{1}{2} \text{Na}_2\text{O}$ to compensate the charge excess due to the insertion of Gd^{3+} ions into the powellite structure. Appropriate amounts of reagents were grounded and calcined at 800°C for 6 hours. Then pellets were obtained with a mechanical press ($P = 350 \text{ MPa}$) and sintered at 1150°C for 15 hours under air, with $5^\circ\text{C}/\text{min}$ rates for heating and cooling.

Heat treatments

Two different crystallization methods were investigated to control the size and the concentration of powellite crystals in the glass-ceramics. Since powellite crystallization is strongly dependent on cooling rates [19, 20], we paid attention to perform all the cooling stages the same way. The nucleation temperature was chosen at 820°C according to literature and differential thermal analysis (DTA) [10, 21, 22]. The growth temperature was chosen at 1050°C.

- (i) The first method consists of a long nucleation stage at 820°C for 110 hours. Samples were placed into a pre-heated furnace and quenched in air. This heat treatment is labeled N (for nucleation).
- (ii) The second method consists of three stages. Samples were placed into a pre-heated furnace for a short nucleation phase at 820°C for 2 hours. The temperature was then raised to 1050°C with an 8°C/min rate for a 20 hours growth stage. After being air quenched, the samples were placed again into the furnace at 820°C for 112 hours. This heat treatment is labeled NG (for nucleation-growth).

The last nucleation stage of the second method was necessary to reach the same powellite concentration obtained during the first heat treatment. Indeed, since the dissolution temperature is close to the nucleation temperature [19], some powellite crystals can dissolve during the growth stage. All samples were annealed at 500°C for 2 hours to release internal stresses.

Samples characterization

EPR measurements were done at room temperature on a X band ($\nu = 9.86$ GHz) EMX Bruker (Wissembourg, France) EPR spectrometer using a 100 kHz field modulation and 3 Gauss of amplitude modulation. Microwave power of 1 mW was used to study Gd^{3+} and Mo^{5+}

ion environments. For EPR line analysis, the line width was calculated between maximum and minimum.

Micro-Raman spectroscopy was performed using a Renishaw INVIA (Wotton-under-Edge, U. K.) spectrometer equipped with a doubled frequency Nd:YAG laser at 532 nm. The laser was focused on the sample using a Leica microscope with a 50X objective, the spectral resolution achievable by the CCD detector is around 2 cm^{-1} . Spectra were recorded between 200 and 1600 cm^{-1} with a 2400 l/mm grating. A linear base line was subtracted from each spectrum which was then normalized to the main peak of powellite. Full Width at Half Maximum (FWHM) of the main powellite peak was calculated after a peak fitting by a pseudo Voigt function.

Chemical analysis of powellite crystals were done on a CAMECA SX 100 electron microprobe analyzer (CAMECA, Gennevilliers, France) equipped with four X-ray spectrometers with an acceleration voltage of 15 kV and a current of 4 nA. Analysis of powellite crystals was conducted on samples obtained by the NG heat treatment since the minimum crystal size needs to be a few micrometers.

Results

Gd³⁺ incorporation in polycrystalline powellite

To better understand Gd³⁺ ions incorporation into the powellite structure, polycrystalline ceramics were characterized by EPR and Raman spectroscopy.

EPR spectra of the ceramics CaMoO₄-Gd and CaMoO₄-Gd-Na are depicted on figure 1. The only paramagnetic species in these ceramics samples is the Gd³⁺ ion (S=7/2). We assumed therefore that all EPR lines could be attributed to the complex fine structure of Gd³⁺ ions (S=7/2) in different environments. Moreover the EPR spectra of Gd-containing powellites is close to spectra of molybdate and tungstate phases containing isolated Gd³⁺ ions

at low content [23]. The study of saturation properties of several EPR lines (not shown here) revealed that Gd^{3+} ions enter the powellite structure with at least three different environments. The comparison of the EPR spectra leads to two important points. First, the area under the EPR spectra is much more important for the ceramic with the charge compensation than for the other ceramic. Since the EPR intensity is proportional to the Gd^{3+} ions concentration, the insertion of these ions into the powellite structure is highly favored by the charge compensation. Second, the EPR lines of the $CaMoO_4$ -Gd-Na ceramic are wider than the ones of the $CaMoO_4$ -Gd ceramic (see zoom on figure 1). This widening could be due to dipole-dipole interaction close to Gd^{3+} ions. Therefore, the Gd^{3+} ions environment is different in the two ceramics. These differences reveal that the insertion of Gd^{3+} ions into the powellite structure was strongly modified by the charge compensation allowed by the Na^+ ions. However, no new EPR lines are observed on the $CaMoO_4$ -Gd-Na spectrum, which means that the Gd^{3+} ions environment is not strongly modified by the presence of Na^+ ions in the structure.

Raman spectra of the three ceramics are given on figure 2. The structure of the spectra is the same as the one commonly reported for scheelite structures [24, 25]. Seven internal modes, corresponding to the vibration of the MoO_4^{2-} tetrahedron, are observed in $CaMoO_4$. The breathing vibration $\nu_1(A_g)$ of the MoO_4^{2-} tetrahedron appears at 878 cm^{-1} . The modes $\nu_3(B_g)$, $\nu_3(E_g)$, $\nu_4(E_g)$ and $\nu_4(B_g)$ are respectively observed at 848, 795, 405 and 393 cm^{-1} . The doubly degenerated modes $\nu_2(A_g + B_g)$ appear around 330 cm^{-1} . All spectra were normalized to the intensity of the main peak at 878 cm^{-1} (called peak A) since it is the less influenced by the beam orientation [26]. All peaks are attributed to $CaMoO_4$ except one, which is only observed if Gd^{3+} and Na^+ ions are in the powellite structure. Indeed, a peak, labeled B, grows around 907 cm^{-1} when Gd_2O_3 and Na_2O oxides are added to pure powellite. Moreover, XRD analysis showed that no secondary crystalline phases are detected in the $CaMoO_4$ -Gd-Na

ceramic. The width of the peak ($\sim 15 \text{ cm}^{-1}$) seems to indicate that it could be linked to a vibration mode of an ion in an ordered environment. A similar peak was reported in literature for polycrystalline powellites enriched with trivalent rare earth elements (Eu^{3+} , Nd^{3+} , La^{3+} , Pr^{3+}) and monovalent charge compensators (Na^+ , Sr^+) [10]. Possible attributions for this unidentified Raman peak will be discussed later.

Gd³⁺ incorporation in CaMoO₄ rich glass-ceramics

The microstructure of the samples from the series Mxg and Mxg1 were studied elsewhere [18]. Depending on the molybdenum and gadolinium contents, samples can either be amorphous or partially crystallized. The results presented here address the incorporation of gadolinium ions in the glassy phase and into the powellite structure.

The evolution of the M25g sample EPR spectrum with heat treatments is plotted on figure 3. The spectra are complex and result from various signals. First, several narrow EPR lines are observed (indexed by arrows on figure 3). They are attributed to Gd^{3+} ions incorporated into powellite structure by comparison with the spectra of ceramics reported on figure 1. Second, we find the well known “U spectrum” with the wide lines at $g = 2$, 2.8 and 6 attributed to Gd^{3+} ions diluted in the glass in network modifier position ($\text{Gd}_{[\text{n.m}]}$) and the line at $g = 4.6$ attributed to Gd^{3+} ions acting as network formers ($\text{Gd}_{[\text{n.f}]}$) [27]. A very wide line is also observed on all EPR spectra, this signal is linked to the formation of magnetic oxide clusters of Gd^{3+} ions, linked through the oxygen bridges [28]. The presence of magnetic clusters was also confirmed by low temperature EPR measurements at 150 K. Finally, a second paramagnetic species was identified, since an extra line at $g = 1.91$ is observed. This line appears only in glasses and glass-ceramics containing MoO_3 and is attributed to Mo^{5+} ions diluted in the glass structure [4, 29, 30]. With increasing the Mo content in parent glasses, the intensity of the line attributed to Mo^{5+} ions increases as already reported in literature [31]. The same trend is observed with the lines attributed to Gd^{3+} ions incorporated

into the powellite structure. This increase is linked to the increase of powellite quantity in the glass-ceramics [18]. After the two heat treatments, some evolutions are visible in the EPR spectrum. First, the signal of Mo^{5+} ions decreases during heat treatments, particularly with the treatment NG during the growth phase at 1050°C . Second, the intensity of lines attributed to Gd^{3+} ions incorporated into the CaMoO_4 structure increases with heat treatments. This evolution seems similar for the two heat treatments and could be due to an increase of powellite quantity and/or to an increase of the incorporation rate during the heat treatments.

EPR spectra of the M25g1 sample (1 mol% Gd_2O_3) before and after heat treatments are given on figure 4. These spectra are quite different from the ones of the M25g sample containing only 0.15 mol% in Gd_2O_3 . First, the intensity of the broad signal due to magnetic oxide clusters of Gd^{3+} ions is far more intense. This means that an important part of the added Gd_2O_3 forms clusters in the glass rather than being part of the glassy network. Indeed the contribution of the “U spectrum” of Gd^{3+} ions involved in the glassy network is similar for the two gadolinium oxide contents. Nevertheless, the line at $g = 4.6$, attributed to Gd^{3+} ions acting as network formers, is no longer visible. The lines attributed to Gd^{3+} incorporated into powellite are also difficult to distinguish but are present. It seems that these lines are very broad, which could be due to dipole-dipole interactions because of a higher incorporation rate. The comparison of the two incorporation rates is, however, not possible because of the complexity of the EPR spectra. This point will be discussed later. Moreover, the line at $g = 1.91$ attributed to Mo^{5+} ions diluted in the glass is barely visible.

Because of the complexity of the spectra, the relative proportion of Gd^{3+} ions incorporated into the CaMoO_4 structure is difficult to calculate. Nevertheless, the mean widths of Gaussian lines attributed to Gd^{3+} ions into powellite can be calculated to compare ions environments. The mean widths were calculated on six Gaussian lines for the series Mxg, Mxg-N and Mxg-NG and are plotted on figure 5. The width for samples from the series Mxg

and Mxg-N are similar whatever the Mo content is. Therefore the Gd^{3+} ions environment is similar in these glass-ceramics. However, the trend is different for the series Mxg-NG. Indeed, the mean width is higher than for samples from the other series and it decreases with the Mo content increase. The ions environments are then different and could be linked to the concentration of inserted ions into the powellite structure.

Raman spectra of samples from the series Mxg-N and Mxg1-N are plotted on figure 6, (a). First, the powellite main peak, A, is broader for the Mxg1-N samples than for the Mxg-N samples. This means that the powellite phase is more disordered when the samples contain more gadolinium. The same observation is made for samples after the NG heat treatment. This trend is better illustrated on figure 7 which depicts peak A FWHM evolution with MoO_3 content (mol%) in glass-ceramics. First, we clearly see that for samples with high content of gadolinium, the peaks are wider than for samples with low content. Second, after NG heat treatment the powellite peak is broader than after N heat treatment. This means that powellite crystals are, on average, more disordered after the NG heat treatment than after the N one. This disorder could be due to a higher incorporation rate of Gd^{3+} ions after the NG heat treatment. Back to figure 6, we observe the peak B, around 907 cm^{-1} , on all samples. The relative intensity of peak B is higher for Mxg1 samples than for Mxg samples, for all thermal histories. This difference could be linked to higher Gd incorporation rates into the powellite structure for samples containing 1 mol% in Gd_2O_3 . To check this point, measurements with an electron probe micro-analyzer (EPMA) were performed on powellite crystals in samples from the Mxg-NG and Mxg1-NG series. After the NG heat treatment, few crystals are large enough to be probed by EPMA. These analyses show that for samples containing 1 mol% in Gd_2O_3 , the average composition of powellite crystals is $Ca_{0.9}Gd_{0.05}Na_{0.05}MoO_4$ whereas it is $Ca_{0.95}Gd_{0.015}Na_{0.015}MoO_4$ for samples containing only 0.15 mol% in Gd_2O_3 . This means that

Gd incorporation rates are higher in samples containing more Gd_2O_3 , which is consistent with EPR and Raman spectra observations. Indeed, figure 8 depicts the evolution of peak A FWHM versus the total substitution rate on the Ca site measured by EPMA. The higher the substitution rate on Ca site is, the larger the peak A is. Moreover, these chemical analyses suggest that the incorporation mode of trivalent lanthanides into powellite structure is accompanied by the insertion of a monovalent ion Na^+ . Therefore, the main incorporation scheme is the replacement of two calcium ions by a gadolinium ion and a sodium ion.

Discussion

In this work, we studied powellite-rich glass-ceramics by EPR and Raman spectroscopy. We showed that gadolinium ions enter the powellite structure and that incorporation rates depend on synthesis processes, gadolinium content in parent glasses and availability of a charge compensator (Na^+). Chemical analyses, like with EPMA, are difficult to use for most of the samples developed during this work. Indeed, the small sizes (few hundred nanometers) and the distribution of crystals in the residual glasses make the analysis often impossible [19]. Therefore, it is very interesting to be able to link spectroscopic parameters, like Raman FWHM or EPR line width, to the incorporation rate into the powellite structure. Raman FWHM is usually linked to the disorder of the crystalline structure. In our case, the disorder is mainly due to the substitution of two calcium ions by a couple (Gd^{3+} , Na^+). For some samples, we demonstrated that Raman FWHM increases with the insertion ratio (cf. fig. 8). Let us assume that the FWHM increase is only due to the increase of the insertion rate. Then powellite crystals obtained by the NG heat treatment have a higher insertion rate than the ones obtained by the N heat treatment. Besides, this higher insertion rate allows us to explain the evolution of EPR lines widths with heat treatment depicted on figure 5. The widening of EPR lines in samples obtained by the NG heat treatment can

therefore be attributed to dipole-dipole interaction between close Gd^{3+} ions in the powellite structure. Even if the analysis of spectroscopic parameters does not give an absolute value of the Gd incorporation rate, it allows us to compare the insertion between the different series and after the heat treatments without the need of uneasy chemical analyses.

During this study, we observed a new peak (peak B) on powellite Raman spectra when Gd^{3+} and Na^+ ions are incorporated into the structure. This peak is also observed on glass-ceramics containing powellite and Gd_2O_3 . Its relative intensity compared to the main peak of powellite increases with the incorporation rate and its FWHM is quite small (around 15 cm^{-1}). According to literature $CaMoO_4$ main peak is usually found between 877 and 879 cm^{-1} [10, 32, 33, 31] and Na_2MoO_4 main peak is found between 891 and 897 cm^{-1} [34, 35]. This peak cannot be attributed to simple molybdates like $CaMoO_4$ or Na_2MoO_4 since its position is 907 cm^{-1} . Therefore, we can assume that the peak B can be attributed to the presence of Gd^{3+} and Na^+ ions incorporated into the powellite. Several assumptions can then be made to attribute peak B. First, we can assume that this peak is due to a secondary phase of general composition $Ca_{1-2x}Gd_xNa_xMoO_4$. The main peaks of phases $CaMoO_4$ and $GdNa(MoO_4)_2$ are respectively at 878 and 882 cm^{-1} [24]. Therefore, the main peak of $Ca_{1-2x}Gd_xNa_xMoO_4$ should be observed between 878 and 882 cm^{-1} . Since peak B is around 907 cm^{-1} , it cannot be attributed to a secondary phase of composition $Ca_{1-2x}Gd_xNa_xMoO_4$ unless its environment is strongly distorted. Indeed, the Mo – O stretching frequency depends strongly on MoO_4^{2-} tetrahedral environment [4]. For instance, the powellite main peak position can increase from 878 cm^{-1} to 900 cm^{-1} if the applied pressure increases from 1 to 8 GPa [36, 32]. A similar trend was observed for the Na_2MoO_4 phase [34]. Second, we can assume that peak B is a splitting of the main peak of powellite. Peak A splitting has been reported in literature by Kolesov et al. for scheelite-like double molybdates $R_{0.5}R'_{0.5}MoO_4$ where R and R' are respectively alkaline and rare earth metals [24]. The splitting of peak A depends on the radius

ratio of R and R' ions and it is attributed to an ordered distribution of these ions in the structure. Other authors, put in evidence ordered distributions in schellite like molybdates by other techniques like XRD, TEM or Monte Carlo simulation [37, 14]. Therefore, peak B could be due to an ordered distribution of Gd^{3+} and Na^+ ions on the octahedral Ca sites in the powellite structure. This assumption allows explaining the fact that no new EPR lines appear when Na^+ ions enter the powellite structure. Indeed, if Na^+ ions are not close enough to Gd^{3+} ions, their structural environment is not strongly modified and no EPR lines appear. In this case, the charge compensation by Na^+ is ensured at a medium or long distance. To conclude on the attribution of peak B, we can reasonably assume that it is due to the insertion of Gd^{3+} and Na^+ ions into the powellite structure with an ordered distribution. Nevertheless, further studies by high resolution TEM and advanced diffraction methods are needed to better characterize the insertion into the powellite structure.

Conclusion

In this work use of EPR and Raman spectroscopy revealed that gadolinium ions are incorporated into the powellite structure in all the glass-ceramics. The incorporation rate strongly depends on the charge compensation by Na^+ ions in pure ceramics. It also depends on the heat treatment and on the initial rare earth concentration in the parent glass for glass-ceramics. Raman spectroscopy suggests an ordered insertion of Na^+ and Gd^{3+} ions into the powellite structure. Nevertheless, further studies on highly doped powellite ceramics with high resolution TEM or advanced XRD Rietveld refinements are needed to better understand the distribution of incorporated elements into powellite.

Acknowledgements

The authors acknowledge Mickaël Bouhier for the help during Raman analyses.

References

- [1] C. Cousi, F. Bart, and J. Phalipou. “Phase separation and crystallization induced by adding molybdenum and phosphorus to a soda-lime-silicate glass”, *Glass Technol.*, 45, 65–67, (2004).
- [2] S. Schuller, O. Pinet, A. Grandjean, and T. Blisson. “Phase separation and crystallization of borosilicate glass enriched in MoO₃, P₂O₅, ZrO₂, CaO”, *J. Non-Cryst. Solids*, 354, 296–300, (2008).
- [3] S. Schuller, O. Pinet, and B. Penelon. “Liquid-liquid phase separation process in borosilicate liquids enriched in molybdenum and phosphorus oxides”, *J. Am. Ceram. Soc.*, 94, 447–454, (2011).
- [4] D. Caurant, O. Majérus, E. Fadel, A. Quintas, C. Gervais, T. Charpentier, and D. Neuville. “Structural investigations of borosilicate glasses containing MoO₃ by MAS - NMR and Raman spectroscopies”, *J. Nucl. Mater.*, 396, 94–101, (2010).
- [5] R.J. Short, R.J. Hand, and N.C. Hyatt. “Molybdenum in nuclear waste glasses - incorporation, and redox state”, *Mater. Res. Soc. Symp. Proc.*, 757, 141–146, (2003).
- [6] Y. Kawamoto, K. Clemens, and M. Tomozawa. “Effects of MoO₃ on phase separation of Na₂O-B₂O₃-SiO₂ glasses”, *J. Am. Ceram. Soc.*, 64, 292–96, (1981).
- [7] E. Cavalli, E. Bovero, and A. Belletti. “Optical spectroscopy of CaMoO₄:Dy³⁺ single crystals”, *J. Phys. Condens. Matter.*, 14, 5221–5228, (2002).
- [8] P. Pascal. *Complément au nouveau traité de chimie minérale*, (1979).

- [9] J. V. Crum, B.J. Riley, L.R. Turo, M. Tang, and A. Kossoy. Summary report: Glass-ceramic waste forms for combined fission products. Technical report, U.S. Department of Energy Waste Form Campaign, (2011).
- [10] C. Mendoza. *Caractérisation et comportement sous irradiation de phases powellites dopées terres rares. Application au comportement à long terme des matrices de confinement des déchets nucléaires*. PhD thesis, Université Claude Bernard, France, 2010.
- [11] V. M. Longo and A. T. de Figueiredo. “Different origins of green-light photoluminescence emission in structurally ordered and disordered powders of calcium molybdate”, *J. Phys. Chem. A*, 112, 8920–8928, (2008).
- [12] V. Morozov, A. Mironov, B. Lazoryak, E. Khaikina, O. Basovich, M. Rossell, and G. Van Tendeloo. “ $\text{Ag}_{1/8}\text{Pr}_{5/8}\text{MoO}_4$: An incommensurately modulated scheelite-type structure”, *J. Solid State Chem.*, 179, 1183 – 1191, (2006).
- [13] D. Bosbach, T. Rabung, F. Brandt, and T. Fanghänel. “Trivalent actinide coprecipitation with powellite (CaMoO_4): Secondary solid solution formation during HLW borosilicate-glass dissolution”, *Radiochimica Acta*, 92, 639–643, (2004).
- [14] V. L. Vinograd, D. Bosbach, B. Winkler, and J. D. Gale. “Subsolidus phase relations in $\text{Ca}_2\text{Mo}_2\text{O}_8$ - $\text{NaEuMo}_2\text{O}_8$ -powellite solid solution predicted from static lattice energy calculations and Monte Carlo simulations”, *Phys. Chem. Chem. Phys.*, 10, 3509–3518, (2008).
- [15] L.H.C. Andrade, M. Siu Li, Y. Guyot, A. Brenier, and G. Boulon. “Optical multi-sites of Nd^{3+} -doped CaMoO_4 induced by Nb^{5+} charge compensator”, *J. Phys. Condens. Matter.*, 18, 7883–7892, (2006).
- [16] M. Schieber and L. Holmes. “Crystal growth and magnetic susceptibilities of some rare-earth sodium molybdenum scheelites”, *J. Appl. Phys.*, 35, 1004–1005, (1964).
- [17] D. Zhao, F. Li, W. Cheng, and H. Zhang. “Scheelite-type $\text{NaEr}(\text{MoO}_4)_2$ ”, *Acta. Cryst.*, E66:i36, (2010).

- [18] T. Taurines and B. Boizot. “Microstructure of powellite-rich glass-ceramics : a model system for high level waste immobilization”, *J. Am. Ceram. Soc.*, 95,1105–1111, (2012).
- [19] M. Magnin. *Etude des processus de démixtion et de cristallisation au sein de liquides fondus borosilicatés riches en oxyde de molybdène*. PhD thesis, Université Pierre et Marie Curie, France, (2009).
- [20] T. Taurines and B. Boizot. “Synthesis of powellite-rich glasses for high level waste immobilization”, *J. Non-Cryst. Solids*, 357, 2723–2725, (2011).
- [21] X. Orhac. *Étude de la stabilité thermique du verre nucléaire. Modélisation de son évolution à long terme*. PhD thesis, Université de Montpellier II, France, (1999).
- [22] N. Henry, P. Deniard, S. Jobis, R. Brec, C. Fillet, F. Bart, A. Grandjean, and O. Pinet. “Heat treatment versus microstructure in molybdenum-rich borosilicates”, *J. Non-Cryst. Solids*, 333, 199–205, (2004).
- [23] E. Tomaszewicz, D. Dąbrowska, S.M. Kaczmarek, and H. Fuks. “Solid-state synthesis and characterization of new cadmium and rare-earth metal molybdatotungstates $\text{Cd}_{0.25}\text{RE}_{0.50}(\text{MoO}_4)_{0.25}(\text{WO}_4)_{0.75}$ (RE = Pr, Nd, Sm - Dy)”, *J. Non-Cryst. Solids*, 356, 2059 – 2065, (2010).
- [24] B. Kolesov and L. Kozeeva. “Raman study of cation distribution in the scheelite-like double molybdates and tungstates”, *Zhurnal Strukturnoi Khimii*, 34, 52–58, (1993).
- [25] S.P.S. Porto and J.F. Scott. “Raman spectra of CaWO_4 , SrWO_4 , CaMoO_4 and SrMoO_4 ”, *Phys. Rev. B*, 157, 716–719, (1967).
- [26] C. Mendoza, G. Panczer, D. de Ligny, I. Bardez-Giboire, S. Schuller, and S. Peugot. “ CaMOO_4 in a molybdenum-rich glass-ceramic: a spectroscopic study” *Ceramic Transactions*, 217, 43–55, (2010).
- [27] S. Simon, I. Ardelean, S. Filip, I. Bratu, and I. Cosma. “Structure and magnetic properties of $\text{Bi}_2\text{O}_3\text{-GeO}_2\text{-Gd}_2\text{O}_3$ glasses”, *Solid State Commun.*, 116, 83 – 86, (2000).

- [28] J. Kliava, I. Edelman, and A. Potseluyko. “EPR and magnetic properties of Gd^{3+} in oxide glasses”, *J. Magn. Magn. Mater.*, 272-276, 1647–1649, (2004).
- [29] R. J. Landry. “ESR and optical absorption study of Mo^{3+} in a phosphate glass”, *J. Chem. Phys.*, 48:1422–1423, (1968).
- [30] O. Cozar, D. A. Magdas, and I. Ardelean. “EPR study of molybdenum-lead-phosphate glasses”, *J. Non-Cryst. Solids*, 354,1032–1035, (2008).
- [31] D. Caurant, O. Majerus, E. Fadel, and M. Lenoir. “Effect of molybdenum on the structure and on the crystallization of $SiO_2-Na_2O-CaO-B_2O_3$ ”, *J. Am. Ceram. Soc.*, 90, 774–783, (2007).
- [32] E. Sarantopoulou, C. Raptis, S. Ves, D. Christofilos, and G. A. Kourouklis. “Temperature and pressure dependence of Raman-active phonons of $CaMoO_4$: an anharmonicity study”, *J. Phys. Condens. Matter*, 14,8925, (2002).
- [33] Chunhua Cui, Jian Bi, and Daojiang Gao. “Room-temperature synthesis of crystallized luminescent $CaMoO_4$ film by a simple chemical method”, *Appl. Surf. Sci.*, 255,3463–3465, (2008).
- [34] C. Luz-Lima, G. D. Saraiva, A. G. Souza Filho, W. Paraguassu, P. T. C. Freire, and J. Mendes Filho. “Raman spectroscopy study of $Na_2MoO_4 \cdot 2H_2O$ and Na_2MoO_4 under hydrostatic pressure”, *J. Raman Spectrosc.*, 41,576–581, (2010).
- [35] V.P. Mahadevan Pillai, T. Pradeep, M.J. Bushiri, R.S. Jayasree, and V.U. Nayar. “Vibrational spectroscopic studies of $FeClMoO_4$, Na_2MoO_4 and $Na_2MoO_4 \cdot 2H_2O/D_2O$ ”, *Spectrochim. Acta, Part A*, 53,867–876, (1997).
- [36] D. Christofilos, G.A. Kourouklis, and S. Ves. “A high-pressure Raman-study of calcium molybdates”, *J. Phys. Chem. Solids*, 56,1125–1129, (1995).

[37] V. Morozov, A. Arakcheeva, G. Chapuis, N. Guiblin, M. Rossell, and G. Tendeloo.
“KNd(MoO₄)₂: A new incommensurate modulated structure in the scheelite family”, *Chem. Mater.*, 18,4075–4082, (2006).

Figure Captions

Fig 1: EPR spectra of ceramics. Dashed line: CaMoO_4 doped with 0.015 mol% of Gd_2O_3 . Dotted line: CaMoO_4 doped with 0.015 mol% of Gd_2O_3 and charge compensated by Na_2O .

Fig 2: Normalized Raman spectra of ceramics. Solid line: pure CaMoO_4 . Dashed line: CaMoO_4 doped with Gd_2O_3 . Dotted line: CaMoO_4 doped with Gd_2O_3 and charge compensated by Na_2O . Inset: zoom on the region $860 - 920 \text{ cm}^{-1}$.

Fig 3: EPR spectra of glass-ceramics containing 2.5 mol% in MoO_3 and 0.15 mol% in Gd_2O_3 . Solid lines correspond to as quenched samples, dashed lines correspond to N heat treatment and dotted lines to NG heat treatment.

Fig 4: EPR spectra of glass-ceramics containing 2.5 mol% in MoO_3 and 1 mol% in Gd_2O_3 . Solid lines correspond to as quenched samples; dashed lines correspond to N heat treatment and dotted lines to NG heat treatment.

Fig 5: Mean width of EPR lines attributed to Gd^{3+} ions incorporated into the powellite phase in samples from the series Mxg, Mxg-N and Mxg-NG. Squares: as quenched samples, circles: samples after N heat treatment and rhombuses: samples after NG heat treatment.

Fig 6: Raman spectra of glass-ceramics in the region $800 - 980 \text{ cm}^{-1}$. (a) Series Mxg-N (solid lines) and Mxg1-N (dotted lines). (b) Series Mxg-NG (solid lines) and Mxg1-NG (dotted lines).

Fig 7: FWHM of the main Raman peak of powellite (peak A at 870 cm^{-1}) after N and NG heat treatments.

Fig 8: Evolution of peak A FWHM with the substitution rate on the Ca site in CaMoO_4 measured by electronic microprobe in glass-ceramics from the series Mxg-NG and Mxg1-NG. The FWHM of a non substituted powellite was measured on a pure polycrystal (square).

Figures

Fig 1

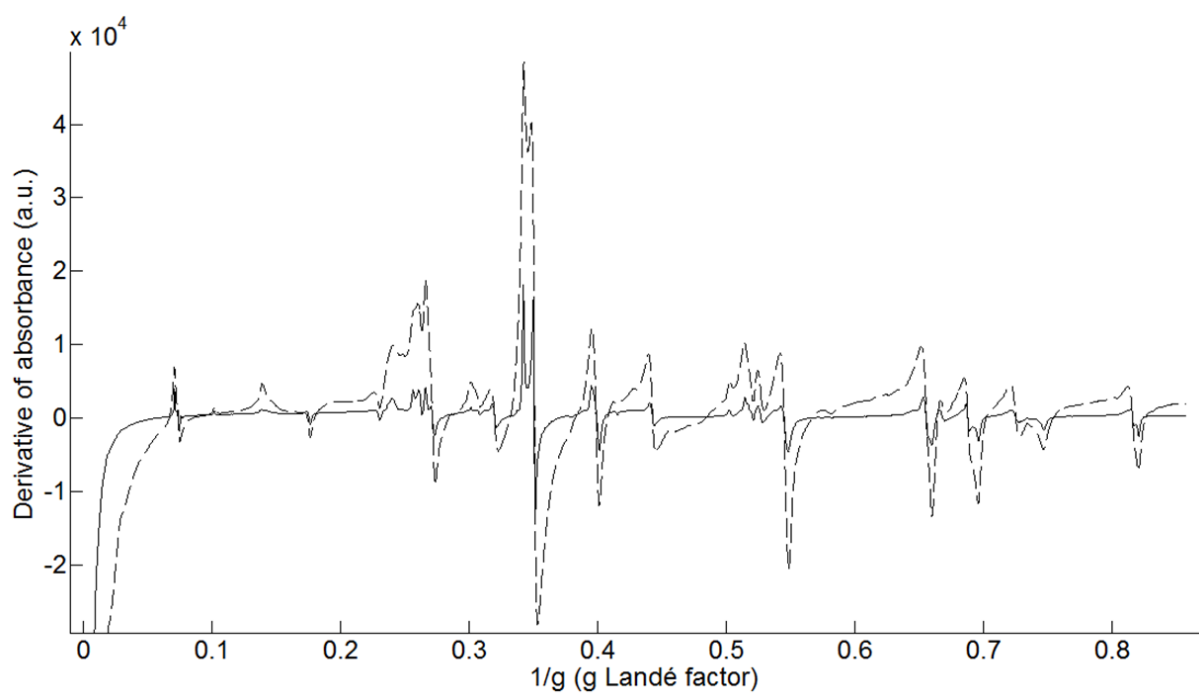


Fig 2

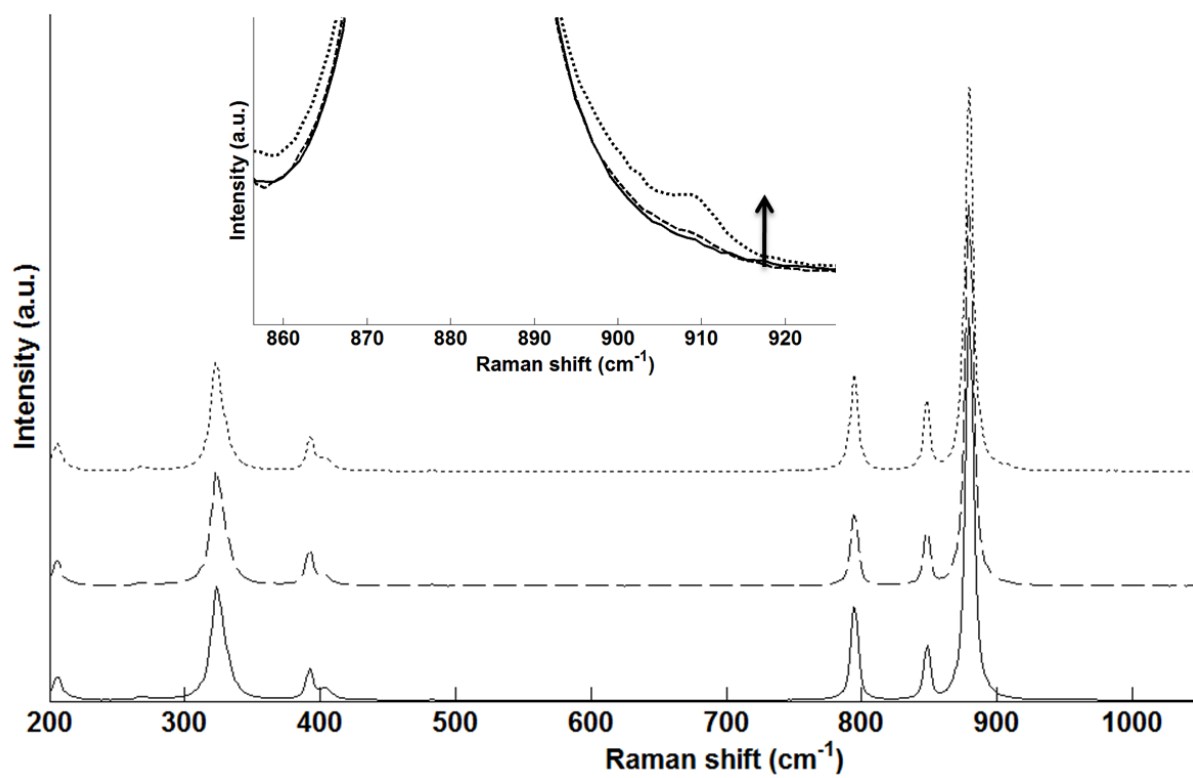


Fig 3

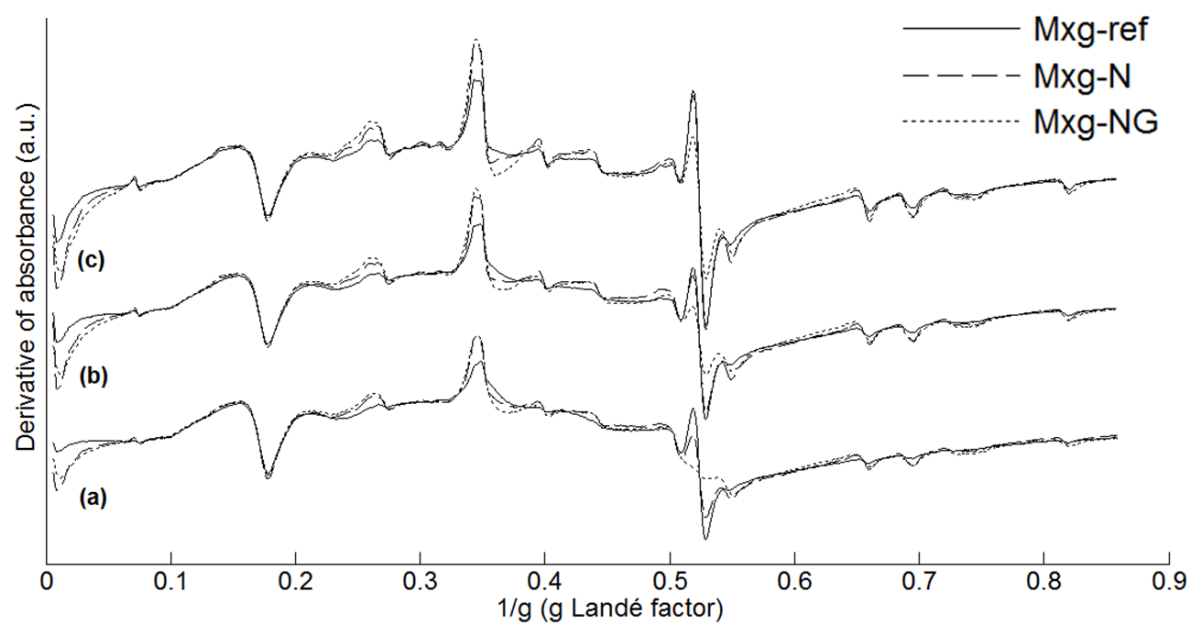


Fig 4

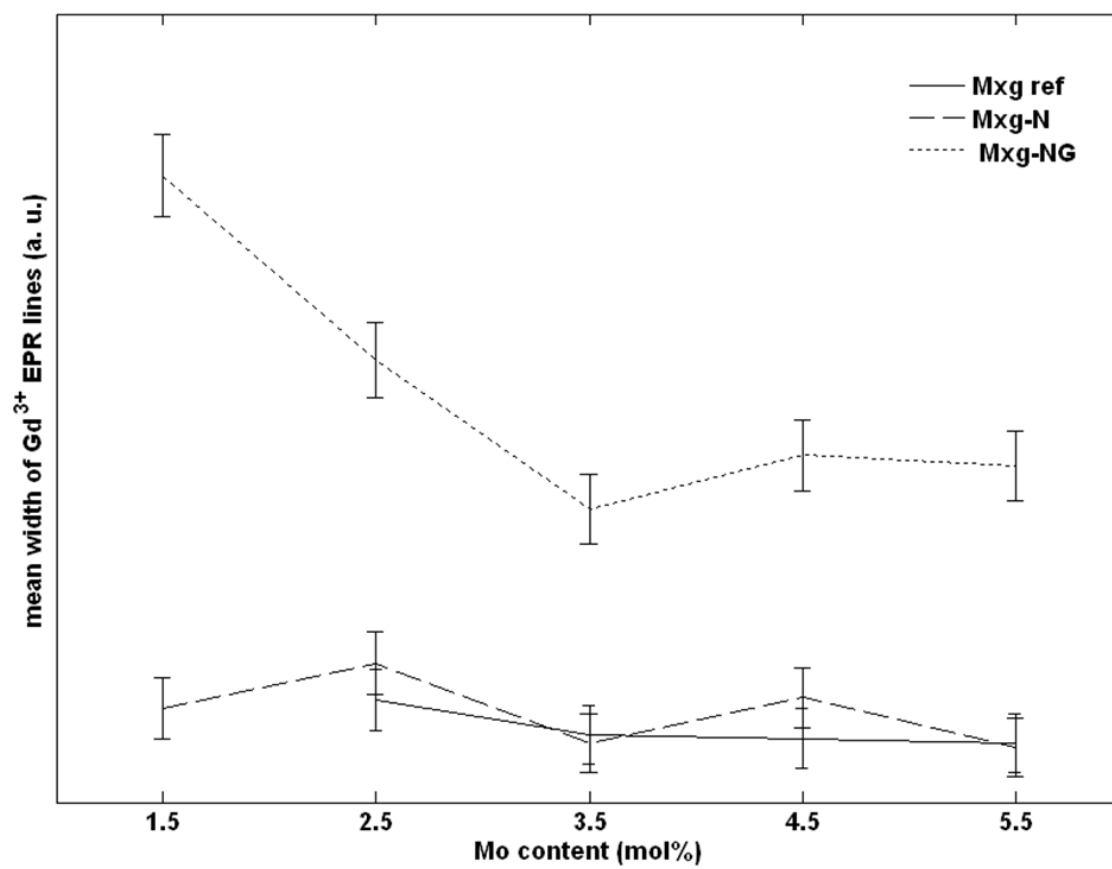


Fig 5

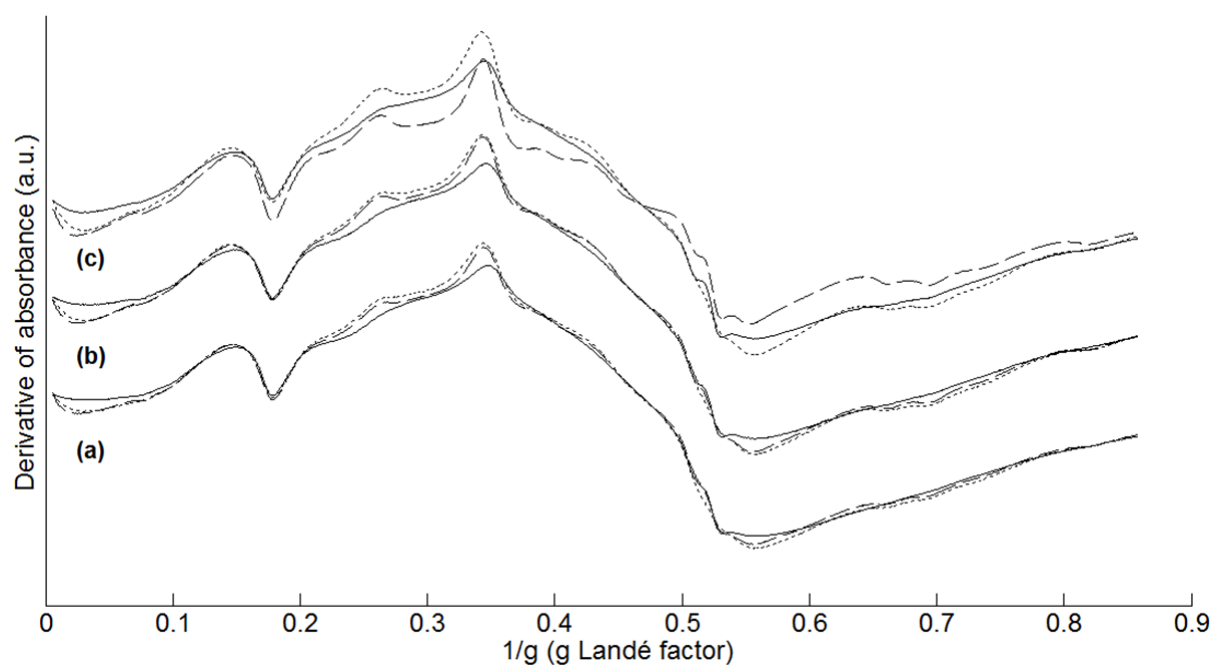


Fig 6

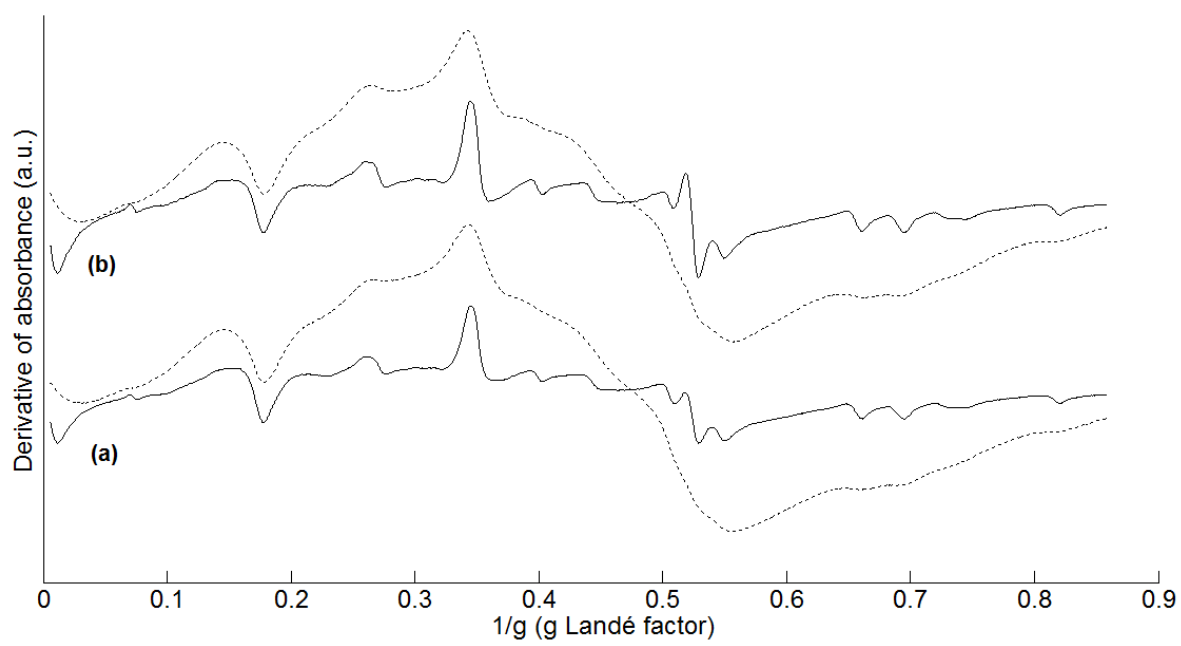


Fig 7

